

Mesocrystal TiO₂ films: In-situ Topotactic Transformation and Application in Dye-Sensitised Solar Cells

Bingyu Lei,^a Arivazhagan Valluvar Oli^b, Aruna Ivaturi^b and Neil Robertson ^{*a}

Supporting Information

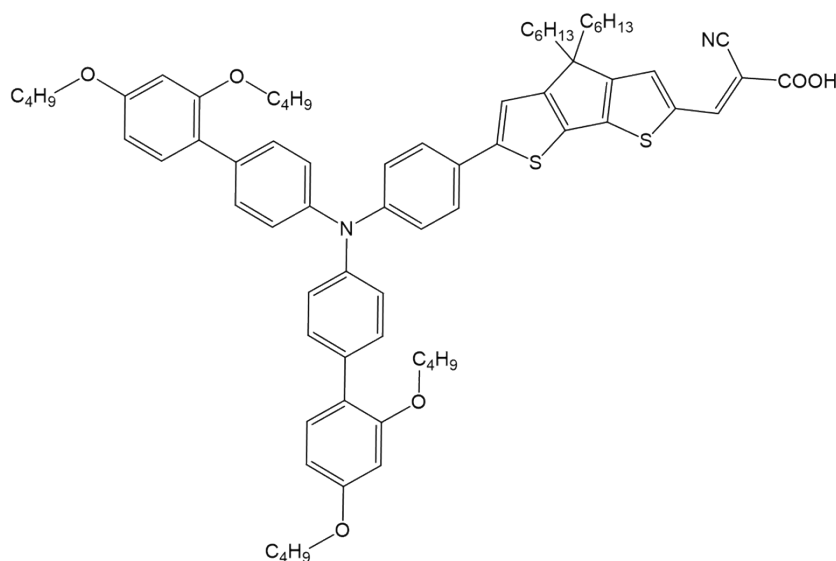


Figure S1: Molecular structure of LEG4.

Table S1: Comparison between NH₄TiOF₃ paste and commercial TiO₂ pastes.

| | NH ₄ TiOF ₃ paste | Ti-Nanoxide T/SP | Ti-Nanoxide D/SP | Ti-Nanoxide R/SP |
|--------------------------------|---|------------------|-----------------------------------|------------------|
| Abbreviation | F | T | D | R |
| TiO ₂ particle size | 200~350 nm | 15-20 nm | 15-20 nm + diffusing particles | >100 nm |
| TiO ₂ concentration | / | ~ 18 wt.% | ~ 18 wt.% | ~ 18 wt.% |
| Ti concentration | ~ 10.8 wt.% | ~ 10.8 wt.% | ~ 10.8 wt.% | ~ 10.8 wt.% |

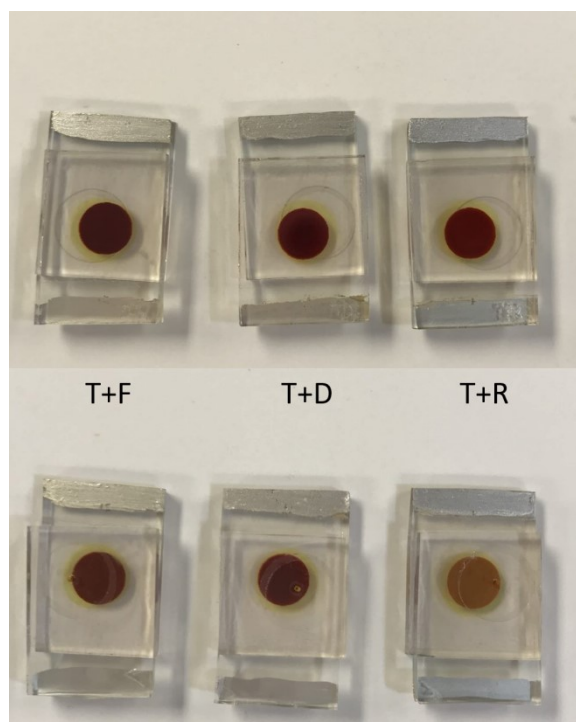


Figure S2 Digital pictures of the example DSSCs from working electrode side (top) and counter electrode side (down). T+F means the photoanode is composed with 1 layer of TiO_2 made from commercial paste Ti-Nanoxide T/SP and 1 layer of TiO_2 made from NH_4TiOF_3 paste. D: Ti-Nanoxide D/SP; R: Ti-Nanoxide R/SP.

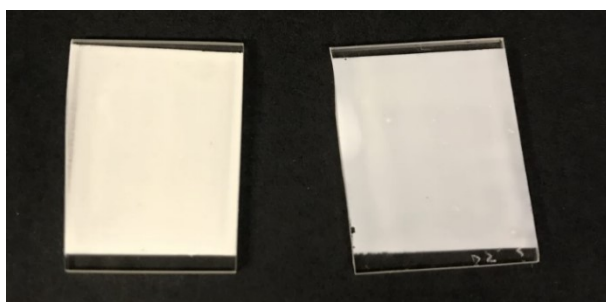


Figure S3 A digital photo of the doctor-bladed films from NH_4TiOF_3 paste (left) or commercial paste Ti-Nanoxide D/SP (right), followed by a sintering process at at $500\text{ }^\circ\text{C}$ for 2 hours with a heating rate of $2\text{ }^\circ\text{C}/\text{min}$

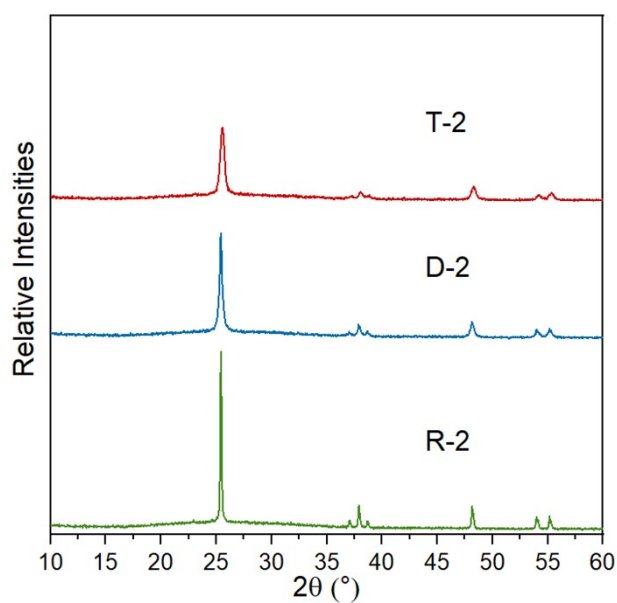


Figure S4: XRD patterns of TiO_2 films from commercial available pastes (Ti-Nanoxide T/SP, Ti-Nanoxide D/SP, Ti-Nanoxide R/SP) sintered at 500 °C for 2 hours with a heating rate of 2 °C/min.

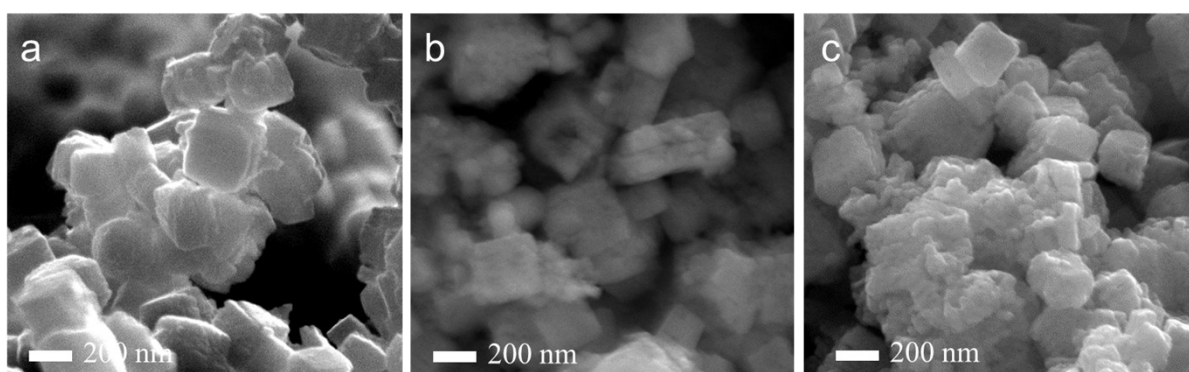


Figure S5: SEM images of mcTiO_2 films from NH_4TiOF_3 paste sintered at 500 °C for 2 hours with different heating rate, namely (a) 1 °C/min, (b) 5 °C/min, (c) 10 °C/min.

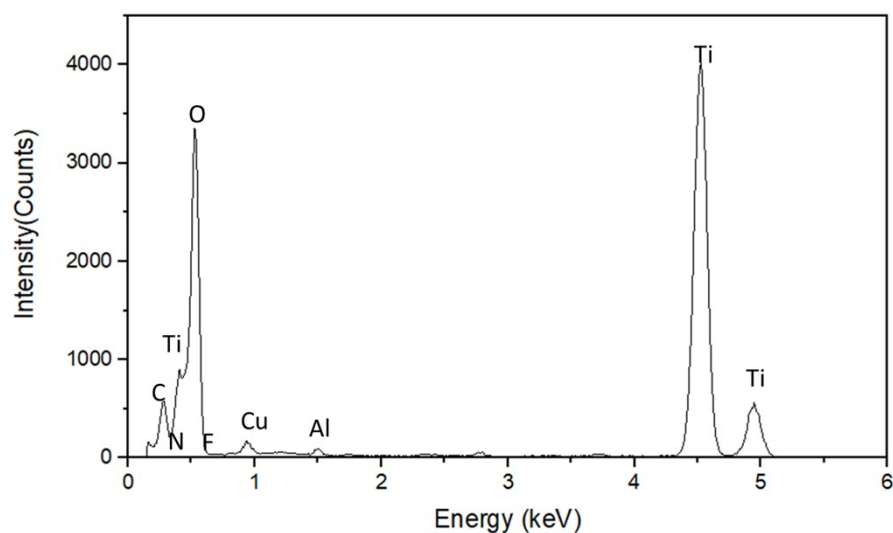


Figure S6: EDS spectrum of mcTiO₂ sintered at 500 °C for 2 hours with a heating rate of 2 °C/min.

Table S2: Elemental composition of mcTiO₂ from TEM-EDS analysis.

| Element | Atomic fraction (%) | Mass fraction (%) |
|---------|---------------------|-------------------|
| N | 1.09 | 0.507 |
| O | 54.5 | 28.9 |
| F | 0.0147 | 0.00928 |
| Ti | 44.4 | 70.6 |

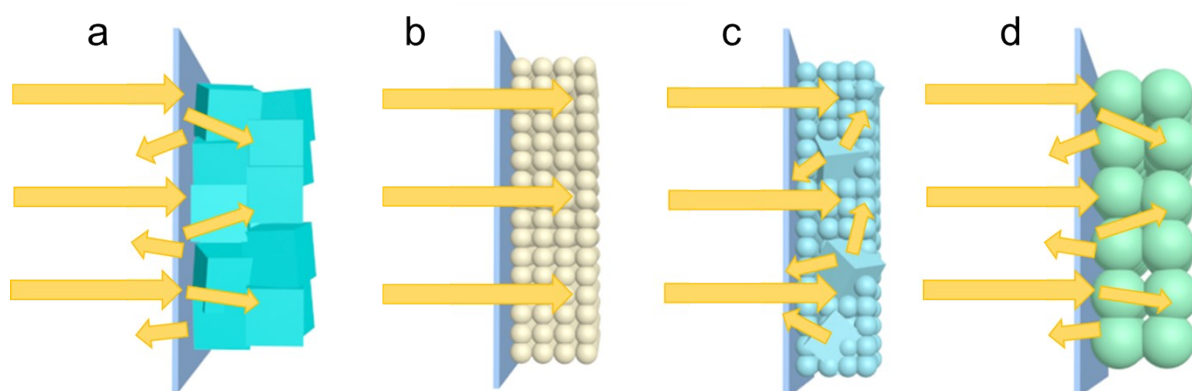


Figure S7: Schematic illustrations of the light path in DSSCs with different TiO₂ as photoanodes. (a) mesocrystal TiO₂ from NH₄TiOF₃ paste, (b) transparent TiO₂ from Ti-Nanoxide T/SP, (c) diffractive TiO₂ from Ti-Nanoxide D/SP, (d) reflecting TiO₂ from Ti-Nanoxide R/SP.

Table S3: Comparison of some EIS parameters between different single-layer photoanodes.

| TiO ₂ | R _s (Ω) | R _{pt} (Ω) | R _{rec} (Ω) | C _μ (μF) | α | β |
|------------------|--|---------------------|----------------------|---------------------|---|---|
| | Fitted parameters from Nyquist plot under -0.7 V bias under white LED illumination | | | | Extracted from lnC _μ v.s. bias | Extracted from lnR _{rec} v.s. bias |
| F | 12.15 | 31.84 | 360.9 | 126.4 | 0.40 | 0.72 |
| T | 13.22 | 44.65 | 244.0 | 192.2 | 0.26 | 0.66 |
| D | 12.58 | 50.79 | 525.6 | 113.3 | 0.30 | 0.61 |
| R | 12 | 60.97 | 2166 | 40.26 | 0.18 | 0.50 |

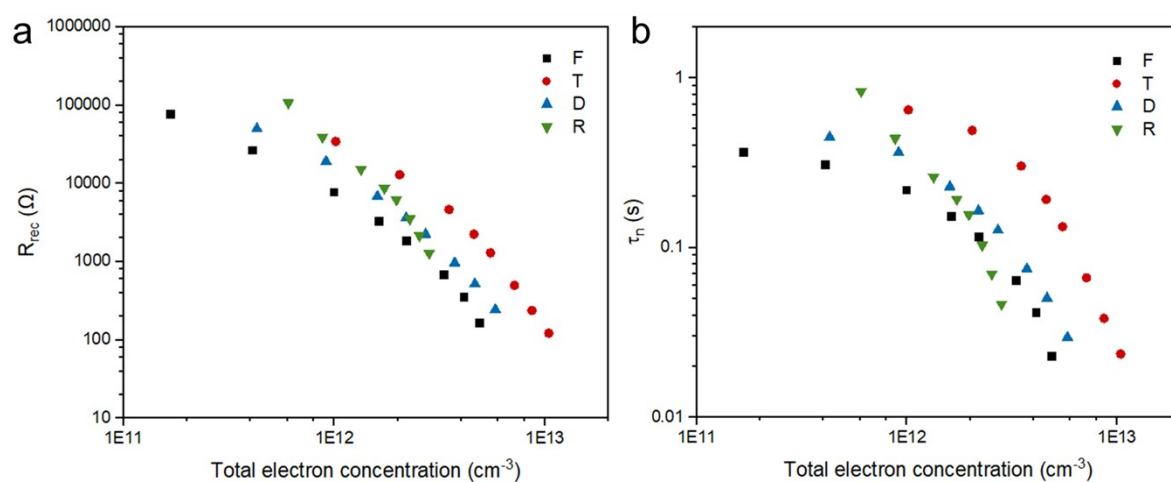


Figure S8: (a) Recombination resistance and (b) electron lifetime of single-layer photoanodes as a function of total electron concentration.

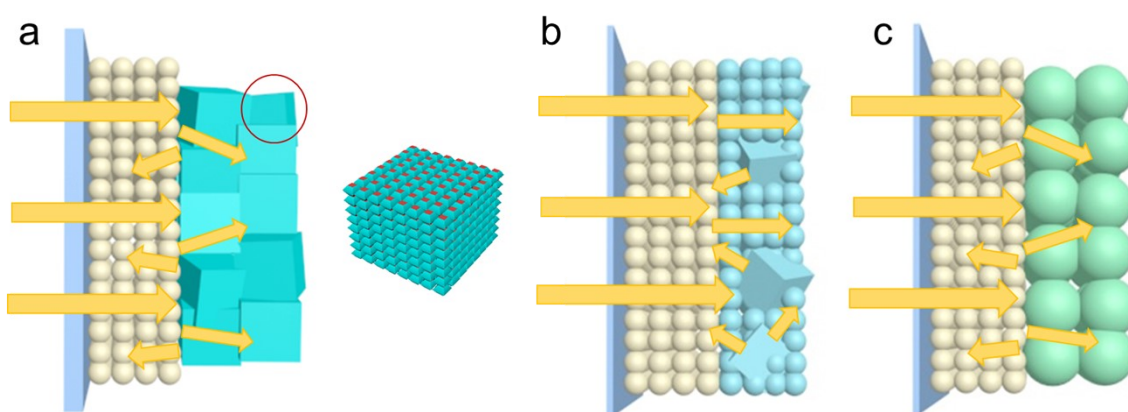


Figure S9: Schematic illustrations of the photoanodes with different scattering layer. (a) mesocrystal TiO₂, (b) diffractive TiO₂, (c) reflecting TiO₂.

Table S4: Comparison of some EIS parameters between different two-layer photoanodes.

| TiO ₂ | α | β |
|------------------|----------|---------|
| T+F | 0.31 | 0.69 |
| T+D | 0.31 | 0.64 |
| T+R | 0.29 | 0.64 |

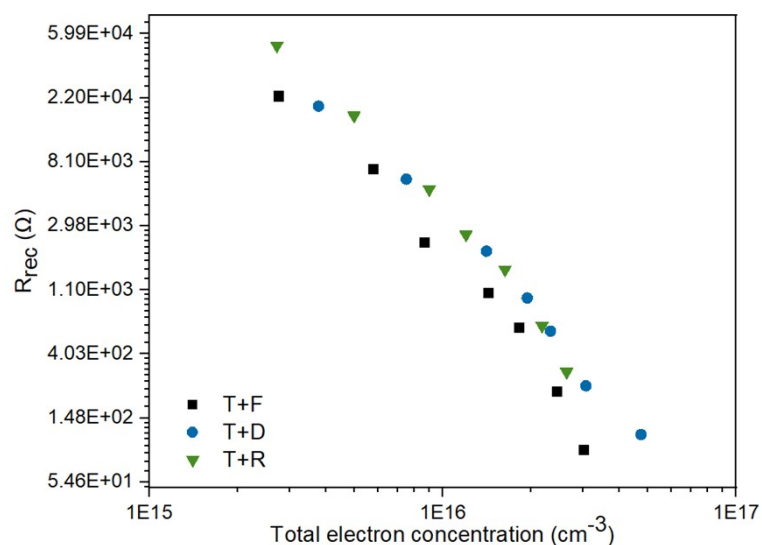


Figure S10: Recombination resistance of two-layer photoanodes as a function of total electron concentration.

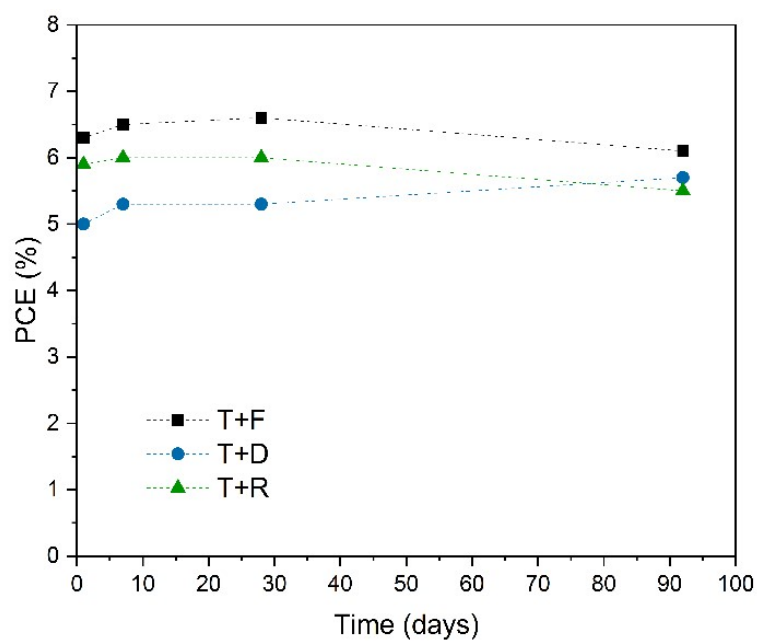


Figure S11 PCE records of DSSCs based on different photoanodes. Devices were kept in dark at the ambient condition.

